Available online at: http://www.basra-science-journal.org

ISSN –1817 –2695

Received 30-9-2015, Accepted 24-3-2015

Photoionization,Electron-Ion Recombination and Radiative Processes of He and Ne Rare Gas Atoms using Relativistic Dirac R-matrix Method

A.H.Hussain A.A.Khalaf F.A.Ali

University of Basrah , College of Science, Department of Physics , IRAQ

e.mail : akeel_hashem74@yahoo.com

Abstract

The Photoionization , Electron -ion recombination and Radiative Processes of He and Ne rare gas atoms are investigated using the fully relativistic R-matrix method . These processes are fundamental atomic processes in astrophysical plasmas. In most existing astrophysical models these atomic data are from methods that do not sufficiently consider the level of complexity attributable to the large number of autoionizing resonances that manifest themselves in the photoionization cross-sections and, consequently, in the inverse process of (electron-ion) recombination.The Dirac Atomic R-matrix Code has been extended from low-energy electron scattering to handle bound states, photoionization and radiative recombination .In the relativistic R-matrix calculations,the sequare integrable orbitals are obtained from the multiconfiguration Dirac-Fock method by using GRASP code,where in this method ,an atomic state is approximated by a linear combination of configuration state functions of the same symmetry.The configuration state functions are antisymmetrized products of a common set of orthonormal orbitals which are optimized on the bases functions of Dirac-Coulomb Hamiltonian.This basis is used to obtain bound orbitals from which the target ions are constructed in DARC code .Further relativistic contributions to the atomic states due to Breit interactions are added by diagonalizing the Dirac-Coulomb-Breit Hamiltonian matrix.The dominant quantum electrodynamic contibutions have also been included as a perturbation.Calculations have been performed on He and Ne rare gas atomic systems,where good agreement is obtained between the results in this paper with the results of others.

Keywords: Photoionization; e-ion recombination; Dirac equation ; relativistic R-matrix method

1.Introduction

During the past years, there has been renewed interest in the photoionization and other radiative processes of atoms and their ions. This interest is, on the one hand, due to the desire of understanding the fundamental atomic processes, on the other hand, due to the need of practical applications in the plasma physics.West[1] gave a review on the development of both theoretical and experimental works on the photoionization of atomic ions over the last 25 years. Opacity project[2-3] obtained a large amount of radiative atomic data to calculate the radiative opacity of the astrophysical plasmas. Collisions of electrons and photons with atoms and ions are among the most elementary processes that can be studied within the framework of quantum mechanics. The latter include elastic scattering, inelastic excitation, and ultimately collisional break-up in ionization. These collisions determine to a considerable extent the energy balance for different plasma and laser devices, while the understanding of the underlying mechanisms allows one to study comprehensively the properties of atomic systems and their structure. Benchmark experiments and calculations have further advanced our basic knowledge of this field, while at the same time providing urgently needed input data for modeling programs describing astrophysical and laboratory plasmas, planetary atmospheres, and lasers. Due to the many difficulties associated with experimental investigations of these collisions, such as the normalization of absolute cross sections and low count rates, and also due to the enormous amount of data needed for the modeling programs, the vast majority of currently available input data for these programs consists of theoretical predictions[4].The photoionization of atomic systems, one of the fundamental processes of nature, also has a myriad of applications to other branches of physics, to other sciences, and to technology generally. Thus, for both basic and applied reasons, atomic photoionization has been of interest for a very long time, even in the era before Einstein's explanation of the photoelectric effect in 1905[5].With the development of quantum mechanics early in the twentieth century came calculations of the photoionization process. These calculations were at the simple analytic hydrogenic [6] and Born approximation level [7] until the 1950s when calculations using more realistic central-field or Hartree–Fock wave functions [8] were employed. Then from the late 1960s, a variety of methods for the calculation of atomic photoionization were developed, which attempted to include, at some level of approximation, the many-body interactions among the electrons of the atom in both the initial (discrete) and final (continuum) states of the photoionization process, i.e. electron correlation[9].The photoionization process is also important in high temperature plasma devices, such as controlled thermonuclear fusion reactors[10], and particularly in high-density inertially confined plasmas[11].Also the Photoionization process is considered to be a useful method to carry out spectroscopical and dynamical investigations on atomic systems, as the information thus obtained is of relatively pure form. This is simply because the photon field couples very weakly with the system to induce minimal perturbation. Moreover, since the final channel comprises of only the photoelectron, the incoming photon being absorbed by the target, the analysis becomes rather simple.Over the last several decades there have been many experimental studies [12] on atomic photoionization to understand the dynamics of the process. In recent times, owing to the advent of experimental technology, a renewed interest is seen in high precision measurements.For a long time, the main obstacle to extensive experimental research at energies as low as x-ray range has been the limitation of discrete characteristic lines from x-ray tubes. Currently available x-ray synchrotron

radiation facilities remove this obstacle and provide the experimentalists with an intense, tunable, and highly polarized x-ray beam[13].Since the R-matrix method has proved to be a remarkably stable, robust and efficient technique for solving the close-coupling equations that arise in electron and photon collisions with atoms and ions [14-16] , in this paper the Dirac atomic R- matrix method adopted to calculate bound states and the process of photoionization and radiative recombination of rare gas atoms . Multiconfigurational Dirac-Fock atomic structure calculations are used to obtain the target models for R-matrix calculations. The low photoelectron energy range that this approximation is applicable to is generally similar to that of the energy levels of the target used in the problem.

R-matrix theory was first introduced in nuclear physics by Wigner [17-18].Around the early 1970s it was realised that this approach could also be used in atomic and molecular physics[19].During the past thirty-five years a series of related R-matrix methods have been published periodically.Building on the important foundational work of Allison [20], Burke [21], Hibbert [22] and Robb [23-24], Berrington et.al. published in 1974 [25] and again in 1978 [26] an influential general program based on the non-relativistic Hamiltonian for calculating electron–atom and electron–ion cross sections as well as general atomic and photoionization cross sections and polarizabilities. This method was extended in 1982 by Scott and Taylor [27] to exploit model potentials and to allow for relativistic effects by including terms from the Breit–Pauli Hamiltonian. A non-exchange version of the non-relativistic method was subsequently published by Burke and Scott [28]. In 1995, an updated version of the general method, to calculate electron–atom and electron–ion collision processes,with options to calculate radiative data and photoionization in either LS-coupling or in an intermediate-coupling scheme, was published by Berrington, Eissner and Norrington [29]. This method was based on two earlier methods [26-27] and included extensions by the Opacity Project [30-31] and the Iron Project team [32]. Zatsarinny [4] published a novel implementation of the R-matrix method with two significant innovations compared to the existing methods: non-orthogonal orbitals are used to represent both the bound and continuum one-electron orbitals; and a set of B-splines are used to define the R-matrix basis functions. The above mentioned methods are primarily concerned with low-energy scattering where the incident energy is insufficient to ionize the target. At intermediate energies, from close to the ionization threshold to several times this energy, modelling of the scattering processes is difficult because account must be taken of the coupling amongst the infinite number of continuum states of the ionized target and the infinite number of target bound states lying below the ionization threshold.

In this paper, we consider the photoionization and e-ion recombination of He and Ne rare gas atoms in the resonance energy region using a relativistic R-matrix method. The R-matrix method for electron—atom and photon—atom interactions has been discussed in great detail by Burke et. al.[33].The present calculations have been carried out by using the fully relativistic R-matrix code DARC [34-35],where the detailed information about DARC [34-35] has been included in the package of the code[36].

In sec.2 ,the theory used in this paper will be introduced , in which the relativistic R-matrix method used to achievement the calculations for present paper ,where the relativistic atomic structure program GRASP is used to obtain bound orbitals from which the target ions are constructed in DARC code. Sec.3, deals with the results obtained by using this method,where the calculations have been performed on He and Ne rare gas atomic systems, the results obtained include the energy of levels ,the oscillator strength (f_{ij}) , radiative rates

(A_{ji}) for an electric dipole allowed transition,line strength (S_{ij}), Photoionization and Photo-recombination cross sections,while the conclusions are given in sec.4 .

2.Theory

The R-matrix method proceeds by partitioning configuration space into two regions
by a sphere of radius $r = a$, where r is the relative coordinate of the scattering electron and the centre of gravity of the target atom or ion. This sphere is chosen to completely envelope the electronic orbitals of the target atom or ion. Hence, in the internal region ($r \le a$) exchange and correlation effects between the scattering electron and the target electrons must be included, whereas in the external region ($r > a$) exchange effects can be neglected and the problem simplifies considerably.

In this method , in the internal region, the 'target' or the 'core' ion is represented by an N-electron system interacting with the (N+1)th electron.The(N+1)th electron may be bound or in the continuum depending on its negative or positive energy (E). A coupled state of the (N +1)-electron system is made from a target state $\Phi = |J^t M^t\rangle$ and a single electron state $\phi = |jm\rangle$ as [36]:

$$A[\Phi,\phi]^{J,M} = \sum_{i=1}^{N+1} \frac{(-1)^{N+1-i}}{\sqrt{N+1}} [\Phi(r_1,\dots,r_{i-1},\dots,r_{i+1},\dots,r_{N+1}),\phi(r_i)]^{J,M}$$
$$= A \sum C(J^t jJ; M^t mM)|J^t M^t\rangle|jm\rangle \quad (1)$$

So A is an asymmetrisation operator to account for electron exchange which ensures that each term is antisymmetric with respect to interchange of the space and spin coordinates of any pair of the N + 1 electrons.The function Φ is the channel function that represents the target state coupled with the spin and angular functions for the scattering electron , ϕ is the continuum basis orbitals for the scattered electron, i.e. the (N + 1)th electron function. Capture states are defined when all N + 1 single particle states are bound,$\theta = A[\Phi,\underline{\phi}]^{J,M}$, and are needed to make the wave function complete. All allowed coupled states for a total angular momentum J and parity π form the basis set Θ_k . The J and M superscripts are omitted from later equations. By the diagonalizing the (N+1)-Hamiltonian matrix $\langle\Theta_k|H^{N+1}|\Theta_{k'}\rangle$ over the internal region an orthonormal set of wavefunctions is obtained that can be written as [36]:

$$\Psi_k = \sum_{ij} c_{ijk}\, A[\Phi_i,\phi_{ij}] + \sum_m d_{mk}\theta_m \quad (2)$$

with eigenvalue E_k^{N+1} and eigenvector (c_{ijk}, d_{mk}) , The coefficients c_{ijk} and $d_{mk}$are determined by diagonalizing the total Hamiltonian of the whole system with the basis set expansion defined by eq.(2),where k is the eigenvector index, j the continuum basis function index for a particular κ value, and i the channel index indicating a pair $(J^t\pi^t,\kappa)$ coupled to get the total angular momentum J and parity π .The θ_m are bound channel functions of the (N+1)-electrons system that account for short range correlation and the orthogonality between the continuum and the bound electron orbitals, i.e. scattered and target electrons.Note that for the continuum functions the radial integrals are over a finite range of integration even though the bra and ket notation is being used.

The total wavefunction which satisfies the time-independent Dirac equation [36]:

$$H^{N+1}\Psi = E\Psi \quad (3)$$

for any energy E is expanded in terms of the basis of eq.(2) as [36] :

$$\Psi_E = \sum_k A_{Ek}\Psi_k \quad (4)$$

The relativistic Dirac Hamiltonian in the Dirac R-matrix method for (N+1) electron target atoms or ions with nuclear charge number Z is given in atomic units by [36]:

$$H^{N+1} = \sum_{i=1}^{M+1}(-ic\alpha.\nabla_i + (\beta-1)c^2 + V(r_i)) + \sum_{j=i+1}^{M+1}\frac{1}{|r_j - r_i|} \quad , \quad (5)$$

where i and j index the individual electrons,the electron rest mass has been subtracted, and α and β are 4×4-dimensional Dirac matrices constructed from Pauli spin and unit matrices defined by [36] :

$$\alpha = \begin{pmatrix} 0 & \sigma \\ \sigma & 0 \end{pmatrix} \ , \ \beta = \begin{pmatrix} I_2 & 0 \\ 0 & -I_2 \end{pmatrix} \quad (6)$$

where the components of σ , σ_x , σ_y and σ_z are 2×2 Pauli spin matrices defined by :

$$\sigma_x = \begin{pmatrix} 0 & 1 \\ 1 & 0 \end{pmatrix} \ , \quad \sigma_y = \begin{pmatrix} 0 & -i \\ i & 0 \end{pmatrix} \ , \quad \sigma_z = \begin{pmatrix} 1 & 0 \\ 0 & -1 \end{pmatrix} \quad (7)$$

and I_2 and I_4 are 2×2 and 4×4 unit matrices, respectively. The first three one-electron terms in the Dirac Hamiltonian are a momentum term, mass term and the electron-nucleus Coulomb attraction. The final two-electron term is the Coulomb electron-electron repulsion. The Hamiltonian matrix element can be split so that angular integrals are calculated using Racah algebra and radial integrals by numerical quadrature. Further relativistic corrections, for example the Breit interaction (a virtual photon exchanged between electrons) and other quantum electrodynamic (QED) corrections, self-energy and vacuum polarisation, are not included in the Hamiltonian. However the eigenvalues of the Hamiltonian may be adjusted to approximate these effects, and providing the changes are small this appears to be a reasonable approach [36].

With large complex systems the computational problem can be drastically reduced by using a model potential to describe the inner closed shell core of electrons. Integrals then only need to be calculated for valence electrons, which form excited states, and continuum electrons. where there are M valence electrons in the target and $V(r)$ is the model potential satisfying the boundary conditions [36]:

$$V(r) \sim -\frac{Z}{r} \ \ when \ r \to 0 \ , \ V(r) \sim -\frac{Z-N}{r} \ \ when \ r \to \infty \quad , \quad (8)$$

Although the basis that will be constructed from one-electron orbitals is reduced in size,the continuum functions have to be orthogonalised with the full set of bound orbitals.

Target N-electron states are labelled by total angular momentum J^t and parity π^t. These states are constructed from linear combinations of configuration state functions (CSFs) which have the same angular momentum and parity. Each CSF defines the principal and angular momentum quantum numbers of each individual electron in the configuration. Thus a target state, or level, can be distinguished by the CSF mixing coefficients and it has a particular energy.

The (N+1)-electron, or target+electron, system is also characterised by total angular momentum J and overall parity π . J is formed by coupling vectorially J^t and j , the total angular momentum of the additional electron. The possible ways of doing this are governed by the triangular relation $|J^t - j| \leq J \leq J^t + j$, where the minimum difference between each J is 1. Then each pair $J\ \pi$ are referred to as a "symmetry".Also the (N + 1)th electron is labelled by quantum number κ which is equivalent to specifying both j and the orbital angular momentum l .($2j + 1 = 2|\kappa|, if\ k < 0\ then\ l = -\kappa\ else\ \kappa > 0\ and\ l = \kappa$). Thus a symmetry of the (N + 1)-system is composed of the possible

"channels" which are labelled by $(J^t\pi^t, \kappa)$ pairs , so the angular momentum and parity will be conserved. In a scattering process the symmetry will be conserved. The channel will not changed for elastic scattering but will for inelastic scattering. It may take the sum of many symmetries for a calculation to converge as the scattering energy increases and with it the number of energetically accessible channels. This corresponds to the familiar partial wave expansion in low energy potential scattering. In photoionisation the symmetry is not conserved. The electric dipole transition process involves absorption of a photon with angular momentum l and a change of parity. Therefore photoionization from a particular bound state restricts the

$$\frac{Q_i(a)}{\mathcal{P}_i(a)} = \frac{b+\kappa}{2ac} \qquad (9)$$

for all i , where $P_i(a)$ and $Q_i(a)$ are the large and small radial component of the continuum electron at the boundary, respectively, and b is an arbitrary constant.

$$\frac{d\mathcal{P}_i}{dr}|_{r=a} = \frac{b}{a}\mathcal{P}_i(a) \qquad (10)$$

By using the Hamiltonian eq.(5) and the boundary conditions eq.(9), an expression for the expansion coefficients is found as [38]:

$$A_{Ek} = \frac{1}{2a(E_k^{N+1} - E)} \sum_i w_{ik}(a)[2ac\, Q_i(a) - (b+\kappa_i)\, P_i(a)] \qquad (11)$$

Where $w_{ik}(a)$ surface amplitudes at the boundary $r = a$. Substitution of $\Psi_E(e + ion)$ expansion in the Dirac equation ,eq.(3) the result are set of coupled equations that are solved using the R-matrix method. The solution is a continuum wave function, Ψ_{fE}^- for an electron at positive energies ($E > 0$) , or a bound state, Ψ_i , at a negative total energy ($E \leq 0$). The complex resonant structures in photoionization and recombination result from channel couplings between continuum channels that are open ($k_i^2 > 0$), and ones that are closed ($k_i^2 < 0$), at electron energies k_i^2 corresponding to the Rydberg series converging on to the target thresholds.

Transition matrix elements for photoionization or electron–ion recombination can be obtained using the bound and continuum wave functions as $|\langle \Psi_B||D_1||\Psi_F\rangle| = \langle \Psi_{jE}^-(\bar{\boldsymbol{k}})||D_1||\Psi_i\rangle$, D_1 is either the dipole length operator or the dipole velocity operator where $D_1^L = \sum_{l=1}^{N+1} r_l$ is the dipole length operator, and $D_1^V = \sum_{l=1}^{N+1} c\,\boldsymbol{\alpha}_l$ is the dipole velocity operator , the sum represents the number of electrons. The transition matrix elements sometimes called reduced dipole matrix elements can be reduced to generalized line strength as [39]:

$$S = \sum_{ljJ} |\langle \Psi_{jE}^-||D_1||\Psi_i\rangle|^2 \qquad (12)$$

Where S related with the reduced dipole matrix elements ,defined in either length form S_L or velocity form S_V ,by the equations (in atomic units) [39]:

number of symmetries in the calculation to two or three.On the other hand , the energy will be also conserved ,where if E^{N+1} is the total energy of the electronic system and E_i^N the energy of the target state coupled to the i th channel then the channel energy of a scattered electron is $\epsilon_i = E^{N+1} - E_i^N$. An open channel has $\epsilon_i > 0$, a closed channel has $\epsilon_i < 0$ and at the channel threshold $\epsilon_i = 0$. For photoionisation by a photon with incident energy ω of an atom in an initial bound state with energy E_0^{N+1} the channel energy is similarly $\epsilon_i = \omega + E_0^{N+1} - E_i^N$,where all channels are closed in a bound state [36]. Then the boundary condition at r = a is chosen as [36]:

The boundary condition reduces in the nonrelativistic limit ($c \to \infty\ or\ \alpha \to 0$) to that of burke et.al. [37]:

$$S_L = \sum_{ljJ} \left| < \Psi_{jE}^{-} | \sum_{j=1}^{N+1} r_j | \Psi_i > \right|^2 \quad (13)$$

$$S_V = \omega^{-2} \sum_{ljJ} \left| < \Psi_{jE}^{-} | \sum_{j=1}^{N+1} \nabla_j | \Psi_i > \right|^2 \quad (14)$$

Where Ψ_i and Ψ_{jE}^{-} are the initial bound state and final continuum state wave functions, respectively.

Dipole transition oscillator strengths $f(b,a)$, and thus transition rates, can be calculated like photo-ionisation cross sections using two R-matrix bound states [36] :

$$f(b,a) = \frac{2C}{3g_a} |\langle \Psi_a || D_1 || \Psi_b \rangle|^2 \quad (15)$$

Where $g_a = 2J_a + 1$ is the statistical weight of the initial state a in jj-coupling. $C = w$ in the length form and $C = w^{-1}$ in the velocity form.

The photoionization cross section is proportional to the generalized line strength in length and velocity forms by equations in atomic units [39]:

$$\sigma_{ij}^{L,V} = \frac{8\pi^2 \alpha\, \omega}{3g_i} S_{L,V} \quad (16)$$

Where g_i is the statistical weight factor of the bound state and ω is the incident photon energy.

Recombination cross sections , can be obtained in length and velocity forms $\sigma_{RC}^{L,V}$ by using the principle of detailed balance or Milne relation as [39]:

$$\sigma_{RC}^{L,V} = \sigma_{ij}^{L,V} \frac{g_i}{g_j} \frac{h^2\omega^2}{4\pi^2 m^2 c^2 v^2} \quad (17)$$

Where g_j is the statistical weight factor of the recombined state and v is the photoelectron velocity.

The radiative decay rate (Einstein's A-coefficient) given by [40] :

$$A_{ji}(a.u.) = \frac{1}{2}\alpha^3 \frac{g_i}{g_j} E_{ji}^2 f(b,a) \quad (18)$$

Where E_{ji} is the energy difference between the initial and final states,

$$A_{ji}(sec^{-1}) = \frac{A_{ji}(a.u.)}{\tau_o} \quad (19)$$

where α is the fine-structure constant and $\tau_o = 2.4191 \times 10^{-17} sec$ is the atomic unit of time [40].

3. CALCULATIONS

The Photoionization and e-ion recombination of He and Ne rare gas atoms are investigated using the fully relativistic R-matrix method.These processes are fundamental atomic processes in astrophysical plasmas. However, rather elaborate and extensive atomic calculations are required in order to compute the related photoionization and recombination in an accurate and self-consistent manner. In most existing astrophysical models these atomic data are from methods that do not adequately consider the level of complexity attributable to the large number of autoionizing resonances that manifest themselves in the photoionization cross-sections and, consequently, in the inverse process of (electron-ion) recombination.The Dirac atomic R-matrix code has been extended from low-energy electron scattering to handle bound states , photoionization and radiative

recombination. A relativistic atomic structure program GRASP is used to obtain bound orbitals from which the target ions are constructed in DARC.Calculations have been performed on He and Ne rare gas atomic systems. Good agreement is obtained between the results in this paper with the results of others.

Photoionization and electron-ion recombination cross sections for He and Ne rare gas atoms are carried out with the determination of target wavefunction. The wavefunction have been obtained by using the GRASP code ,The present calculations have been carried out by using the relativistic R-matrix code DARC [34-35].The author of the DARC code is preparing a manual to be published and he suggested that the above references for the DARC. However, the detailed information has been included in the package of the code[36].The Dirac R-matrix theory is based on the Dirac atomic structure code known as GRASP,where is an acronym for the General-purpose Relativistic Atomic Structure Program developed by Grant et. al. ,the version of GRASP is included as a DARC module where adopted in present calculations [36]. This is a fully relativistic code, and is based on the jj coupling scheme. Additionally, the option of extended average level (EAL) are used , in which a weighted (proportional to $2j+1$) trace of the Hamiltonian matrix is minimized. This produces a compromise set of orbitals describing closely lying states with good accuracy [41].

Helium, along with the other noble gases, is both one of the most thoroughly studied systems experimentally and theoretically, experimentally, an important paper was published by West and Marr [42] which gives data for the noble gases obtained using synchrotron radiation.

The wave function for target or core ion He II includes the ground state $n=1$ and excited states of He II from $n=2$ and $n=3$, where the configurations for target or core ion HeII is $(1s^1, 2s^1, 2p^1, 3s^1, 3p^1, 3d^1)$ give rise to 9 fine-structure levels of He II, as given in Table (1). The wave functions of the bound orbitals for the He^+ (sometimes refer it as He II) core have standard analytic expressions for both relativistic and non-relativistic calculations but for convenience the Dirac wave functions were calculated using GRASP.The initial ground state of He has total $J=0$ and even parity. The final state of the $He^+ + e^-$ system has total $J=1$ and odd parity. The configurations of the core ion in the relativistic calculation are formed from Dirac-Hartree-Fock orbitals from a GRASP EAL (extended average level) calculation with nine relativistic configurations.

Table (1) shows the energies of the levels obtained and quantum electro-magnetic (QED) corrections compared with the levels of the calculation of Erickson[43]. The QED correction are not included in the photoionization calculation. Erickson's calculation for $^2He^4$ II includes mass dependency, relativistic, QED and nuclear size effects. The difference between GRASP's and Erickson's results is less than 0.00007%.

Table (2) compares the same energy levels of the target ion for the GRASP EAL calculation,with the DARC configuration interaction (CI) calculation by using the Dirac orbitals and with those obtained from the atomic structure code AUTOSTRUCTURE[44].The three sets of calculations are in very good agreement .

Table (1) : Terms and ground state energy and excitation energies in a.u. for He II in the eigenfunction expansion of He I with QED corrections from GRASP and calculation of Erickson[43].

Term	Parity	J	GRASP	QED $x10^{-5}$	Erickson [43]
1s(^{2}S)	even	1/2	-2.000106	1.4001	-1.99981500
2$\bar{p}$(^{2}P)	odd	1/2	1.500073	-1.4032	1.49985300
2s(^{2}S)	even	1/2	1.500073	-1.2209	1.49985100
2p(^{2}P)	odd	3/2	1.500099	-1.3969	1.49987700
3s(^{2}S)	even	1/2	1.777872	-1.3468	1.77761300
3$\bar{p}$ (^{2}p)	odd	1/2	1.777872	-1.4010	1.77761200
3p(^{2}P)	odd	3/2	1.777880	-1.3991	1.77762029
3$\bar{d}$(^{2}D)	even	3/2	1.777880	-1.4001	1.77762028
3d(^{2}D)	even	5/2	1.777882	-1.4001	1.77762291

Table (2) : Ground state energy and excitation energies in a.u. for He II for GRASP , DARC and AUTOSTRUCTURE [44].

Index	Term	Parity	J	GRASP	DARC	A.S.[44]
1	1s(^{2}S)	even	1/2	-2.000106514	-2.000106529	-2.00010653
2	2$\bar{p}$(^{2}P)	odd	1/2	1.50007323	1.50007378	1.50007327
3	2s(^{2}S)	even	1/2	1.50007323	1.50007378	1.50007329
4	2p(^{2}P)	odd	3/2	1.50009986	1.50009987	1.50009989
5	3s(^{2}S)	even	1/2	1.7778724	1.77787261	1.77787249
6	3$\bar{p}$ (^{2}p)	odd	1/2	1.77787246	1.77787261	1.77787248
7	3p(^{2}P)	odd	3/2	1.77788035	1.77788035	1.77788037
8	3$\bar{d}$(^{2}D)	even	3/2	1.77788035	1.77788035	1.77788036
9	3d(^{2}D)	even	5/2	1.77788289	1.77788299	1.77788299

The absorption oscillator strength (f_{ij}) and radiative rate (A_{ji}) for an allowed transition $i \rightarrow j$ are related by eq.(18),where S is the line strength for E1 transition. Table (3) shows the present transition energies ΔE_{ij}(Ang.), oscillator strengths f_{ij} , radiative rate $A_{ji}(\sec^{-1})$ and line-strength S_{ji} (a.u.) obtained from GRASP in length form only, for all 15 allowed transitions among the 9 levels of He^+. The present results are compared with the results obtained by using the atomic structure code AUTOSTRUCTURE [44] as listed in table (3),where the two sets of calculations are in very good agreement, the indices used to represent the lower and upper levels of a transition have been defined in table (2),while calculating the oscillator strengths and radiative rates, the QED corrected theoretical energies are used as listed in table (1).

Table (3) : Transition energies ΔE_{ij}(Ang.), radiative rates A_{ji}($\sec^{-1}$) ,oscillator strengths f_{ij} and line-strength S_{ji}(a.u.) obtained from GRASP are compared with the results obtained by using the AUTOSTRUCTURE [44] code

			GRASP			AUTOSTRUCTURE		
i	j	ΔE_{ij}	A_{ji}	f_{ij}	S_{ji}	A_{ji}	f_{ij}	S_{ji}
1	2	6.84E+02	1.00E+10	1.39E-01	2.77E-01	1.003E+10	1.385E-01	2.77E-01
1	4	6.84E+02	1.00E+10	2.77E-01	5.55E-01	1.003E+10	2.774E-01	5.547E-01
1	5	8.10E+02	2.68E+09	2.64E-02	4.45E-02	2.676E+09	2.635E-02	4.446E-02
1	7	8.10E+02	2.68E+09	5.27E-02	8.90E-02			
2	6	1.27E+02	3.37E+07	1.36E-02	1.47E-01	3.36E+07	1.358E-02	1.46E-01
2	8	1.27E+02	8.63E+08	6.96E-01	7.51E+00			
3	4	1.21E-02	9.10E-04	7.99E-05	9.00E+00	9.067E-04	7.98E-05	8.999E+00
3	5	1.27E+02	3.59E+08	1.45E-01	1.57E+00	3.593E+08	1.44E-01	1.564E+00
3	7	1.27E+02	3.59E+08	2.90E-01	3.13E+00			
4	6	1.27E+02	6.74E+07	1.36E-02	2.94E-01	6.736E+07	2.71E-02	2.934E-01
4	8	1.27E+02	1.72E+08	6.96E-02	1.50E+00			
4	9	1.27E+02	1.04E+09	6.26E-01	1.35E+01	1.035E+09	1.25E+00	1.352E+01
5	8	3.60E-03	8.88E-05	8.88E-05	3.37E+01			
6	7	3.60E-03	1.42E-04	1.42E-04	5.40E+01			
7	9	1.20E-03	3.94E-06	2.66E-05	6.07E+01			

Figure (1) shows the total photoionization cross section in the length and velocity gauge.In the present calculations the number of continuum orbitals per angular momentum (variable NRANG2) is equal to 15.0 , R-matrix boundary equal to 21.92 a.u. and the arbitrary constant b is zero. For comparison with the He ground state the calculated ionization energy by DARC is 0.88105 a.u. compared with the experimental ionization energy is 0.9033 a.u.[45] .The photon energy range of 4.0 to 8.0 rydberg covers all the thresholds in the He^+ targets, and the resonances of the dominant Rydberg series can be seen clearly. Interestingly though it is the velocity gauge results that seem to be converging on the experimental values of West and Marr [42], whereas the length results slightly are above them.There is excellent agreement between the present results and the theoretical results of Nahar [46],this agreement is due to core excitations,where they are formed due to doubly excited Rydberg states converging to core thresholds (e.g. n=2 for He).So the agreement is satisfactory for the these target states calculations.The closeness of the length and velocity cross sections is usually taken as a sign of accuracy of the representation of the wave functions.

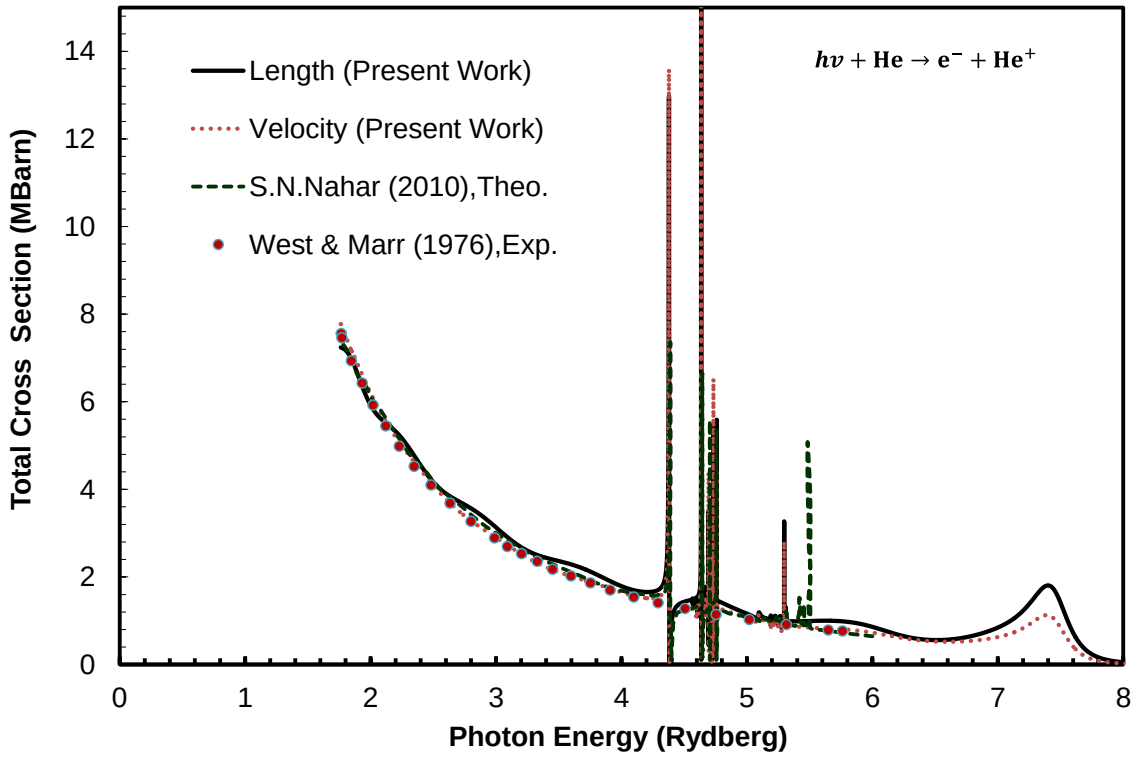

Figure (1) : Total photoionization cross section of He in the length and velocity gauge. using 9 target states.

The computations for the inverse processes of photoionization and electron-ion recombination were carried out through various stages of the Dirac R-matrix codes (DARC) [34-36]. So,according to the previous results of photoionization cross section of He ,the recombination cross sections , can be obtained in length and velocity forms $\sigma_{RC}^{L,V}$ by using eq.(17), according to the principle of detailed balance or Milne relation [39]. Figure (2) shows the total recombination cross section of ($e^- + He^+ \rightarrow He + h\nu$) processes in the photon energy range of 0 to 10.0 rydberg ,the comparision made between length and velocity gage only ,there is a very good agreement for the these target states calculations which covers the thresholds in the He^+ targets.

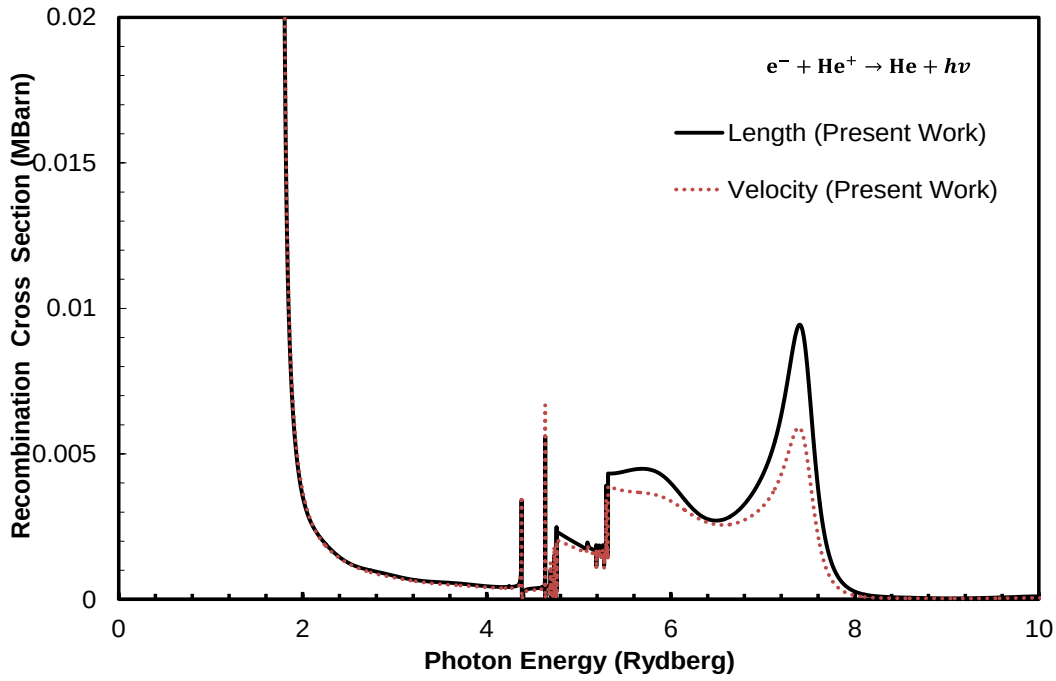

Figure (2) : Total recombination cross section of ($e^- + He^+ \rightarrow He + h\nu$) in the length and velocity gauge using 9 target states.

The Ne atom is used to demonstrate the R-matrix methods consistent approach to resonant and non-resonant regions, in comparison with the large number previous theoretical approaches. There also exists a large amount of accurate experimental data on neon,current high resolution synchrotron radiation studies are continuing to provaid current computations, including R-matrix, to their limits. There are so many publications on the photoionization of Ne for example the Opacity Project by Hibbert and Scott [47].Previously, a standard reference on experimental data for the total photoionization cross section of Ne atom were the tabulated fits to the results of synchrotron measurements by West and Marr [42].

The wave function for target or core ion Ne II includes the configurations ($1s^2 2s^2 2p^5$ and $1s^2 2s^1 2p^6$) leads to 3 fine-structure levels of Ne II, as given in Table (4).The initial ground state of Ne has total $J = 0$ and even parity. The final state of the $Ne^+ + e^-$ system has total $J = 1$ and odd parity.The configurations of the core ion in the simplest relativistic calculation are formed from Dirac-Hartree-Fock orbitals from a GRASP EAL calculation with only three relativistic configurations. Table (4) shows the energies of the levels obtained by GRASP and QED plus Breit corrections compared with the energy levels obtained by DARC. The number of continuum basis functions used to represent each continuum electron with quantum number κ which is equivalent to specifying both j and the orbital angular momentum l .($2j + 1 = 2|\kappa|, if\ k < 0\ then\ l = -\kappa\ \ else\ \kappa > 0\ and\ l = \kappa$), NRANG2, is 25. The boundary radius a, is 5.40 a.u. such that all bound orbitals are less than 10^{-6} in the external region. The arbitrary constant b is zero,where the DARC R-matrix Ne ground state energy is 0.7688 a.u. below the threshold of the Ne+

ground state, compared with 0.7925 a.u. for the experimental ionization energy [45].

Table (5) compares the energy levels of the target ion Ne II for the GRASP EAL calculation,also the DARC CI calculation using the Dirac orbitals , with those obtained by using the atomic structure code AUTOSTRUCTURE[44] and the experimental values from Moore [45].The four sets of states are in good agreement .

Table (4) : Terms, ground state energy and excitation energies in a.u. for Ne II,for GRASP, Breit with QED corrections and DARC.

Index	Term	Parity	J	GRASP	Breit + QED	DARC
1	$2s^2 2\bar{p}\ ^2 2p^3\ (^2P)$	odd	3/2	-127.9645880	0.02605	-127.96457597
2	$2s^2 2\bar{p}^1 2p^4\ (^2P)$	odd	1/2	0.003810211	-0.00030794	0.003806465
3	$2s^1 2\bar{p}\ ^2 2p^4 (^2S)$	even	1/2	1.09065862	-0.00031300	1.09065156

Table (5) : Ground state energy and excitation energies in a.u. for Ne II for GRASP , DARC , AUTOSTRUCTURE [44] and the Moore[45] experimental results.

Term	Parity	J	GRASP	DARC	A.S.[44]	Moore
$2s^2 2\bar{p}\ ^2 2p^3\ (^2P)$	odd	3/2	-127.9645880	-127.96457597	-127.84743161	
$2s^2 2\bar{p}\ ^1 2p^4\ (^2P)$	odd	1/2	0.003810211	0.003806465	0.004640845	0.00356
$2s^1 2\bar{p}\ ^2 2p^4\ (^2S)$	even	1/2	1.09065862	1.09065156	1.08176042	0.98895

For Neon,the absorption oscillator strength (f_{ij}) and radiative rate (A_{ji}) for an allowed transition ($i \to j$) are related by eq.(18),where S is the line strength for electric dipole (E1) transition.Table (6) shows the present transition energies ΔE_{ij}(Ang.), oscillator strengths f_{ij} , radiative rate $A_{ji}(\sec^{-1})$ and line-strength S_{ji} (a.u.) obtained from GRASP [34-36] in length form only, for all 2 allowed transitions among the 3 levels of Ne^+ion,these results compared with the results obtained by using the atomic structure code AUTOSTRUCTURE [44],where the AUTOSTRUCTURE [44] results obtained by using the theoretical transition energies and the same configurations for target ion Ne II that were employed to determine the energies for AUTOSTRUCTURE[44] as listed in table (5).The present results obtained by using the fully relativistic GRASP code [34-36],some of AUTOSTRUCTURE[44] results agree well with the GRASP calculations, but for other transitions, they have the same behavior with transition energy.The two sets of calculations therefore are in satisfactory agreement. The indices used to represent the lower and upper levels of a transition have been defined in Table (4). Also, while calculating the oscillator strengths and radiative rates, the Breit plus QED corrected theoretical energies are used as listed in Table (4) .

Table (6): Transition energies ΔE_{ij}(Ang.), radiative rates $A_{ji}(\sec^{-1})$,oscillator strengths f_{ij} and line-strength S_{ji}(a.u.) for Ne II for GRASP and A.S. [44] .

		GRASP				A.S.		
i	j	ΔE_{ij}	A_{ji}	f_{ij}	S_{ji}	A_{ji}	f_{ij}	S_{ji}
1	3	496.95	1.3455E+10	1.7602E-01	9.6831E-01	1.388E+10	3.6905E-01	1.023465
2	3	495.22	6.6451E+09	1.7509E-01	4.8329E-01	6.849E+09	1.8375E-01	0.511732

Figure (3) and (4) show the total photoionization cross section in the length and velocity gauge.The photon energy range of 3.0 to 4.0 rydberg covers all the thresholds in the Ne^+ targets, and the resonances of the dominant Rydberg series can be seen clearly. Interestingly though it is the length gauge results that seem to be converging on the length gauge results.There is a good agreement between

the present results and the theoretical results of both Yeh and Lindau [48] and Verner and Yakovlev [49].By increasing the photon energies the results between length and velocity converging with each other. The results of Yeh and Lindau [48] and Verner and Yakovlev [49] neglect the fine structure of atomic levels therefore the resonances positions disappear ,while in the present results they are formed due to doubly excited Rydberg states converging to core thresholds.In general, except for the resonances positions the shape of curves exhibit behavior comparable to the present results.Therefore the agreement is satisfactory for the present target states calculations,where the photoionization cross sections are sensitive to target energy levels.The closeness of the length and velocity cross sections is usually taken as a sign of accuracy of the representation of the wave functions.

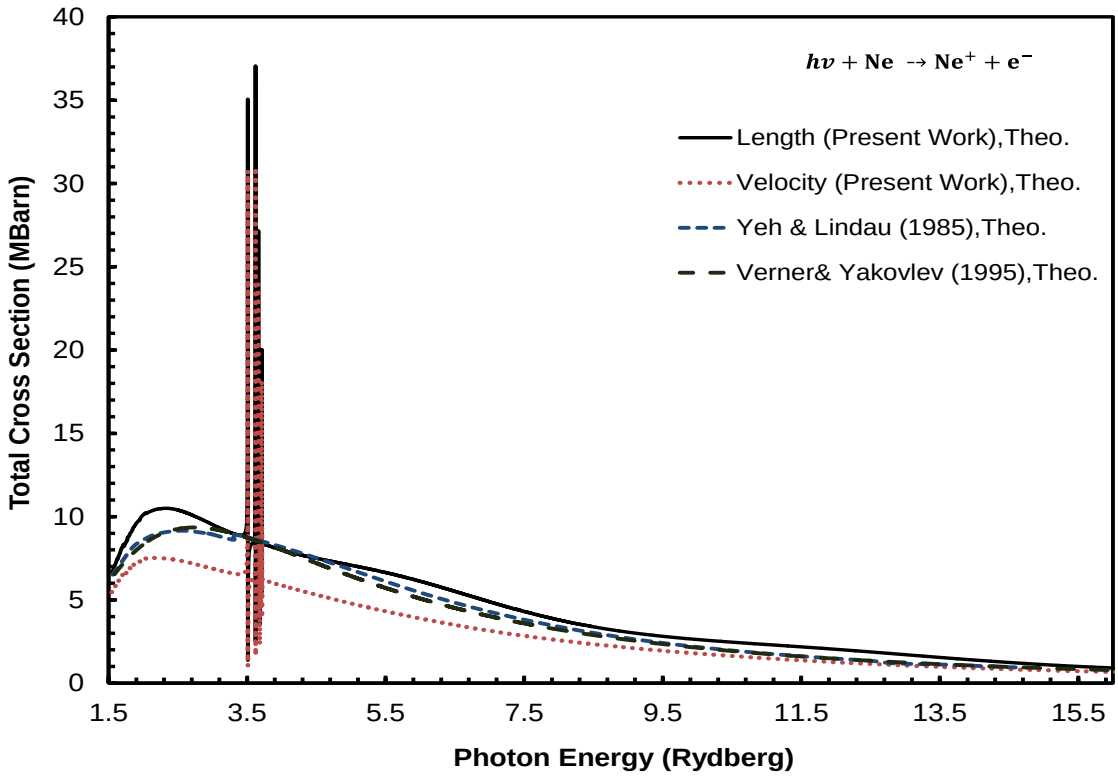

Figure (3) : Total photoionization cross section of Ne in the length and velocity gauge. using 3 target states.

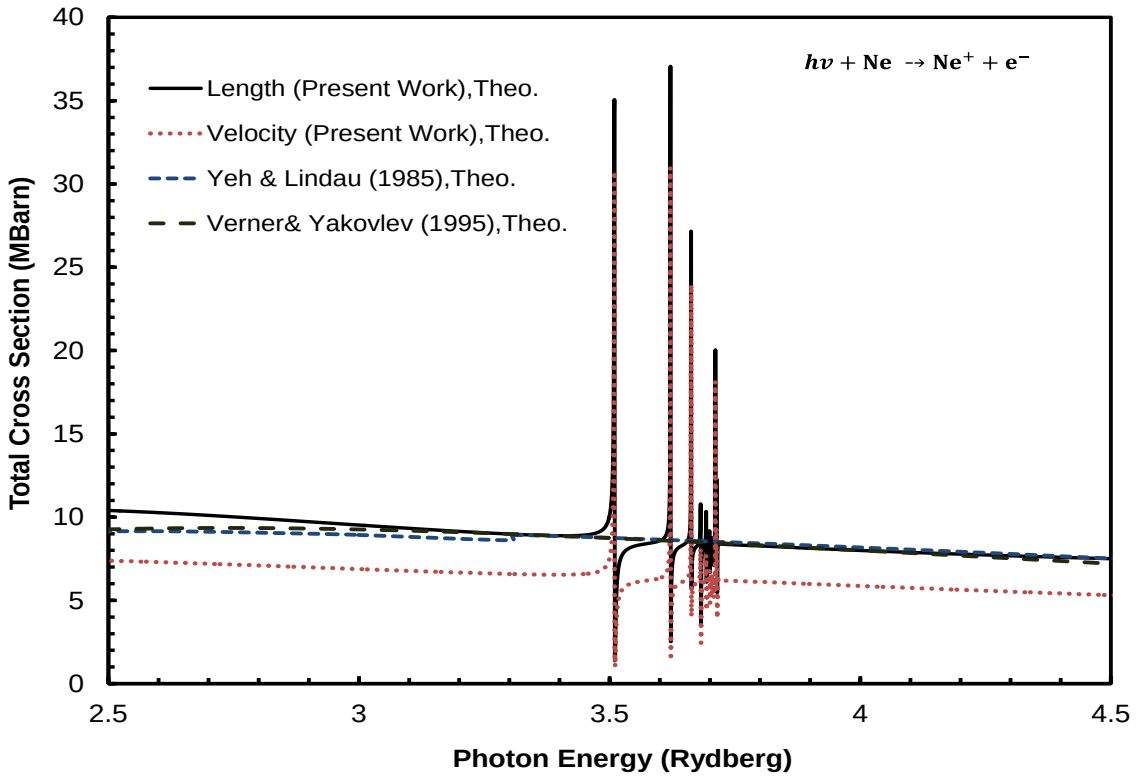

Figure (4) : Expansion of figure (3) .

According to the present results for photoionization cross section of Ne,the recombination cross section related to the photoionization cross section and can be obtained in length and velocity forms $\sigma_{RC}^{L,V}$ by using eq.(17), according to the principle of detailed balance or Milne relation [39]. Figure (5) shows the total recombination cross section of $(e^- + Ne^+ \rightarrow Ne + h\nu)$ processes in the photon energy range of 1.5 to 16 rydberg,while figure (6) is expansion of figure (5) where recombined state can be seen clearly in the photon energy range of 3.5 to 3.71 rydberg .The comparisions made between length and velocity gage only, the length results are slightly above the velocity results,in general there is a good agreement for the these target states calculations.

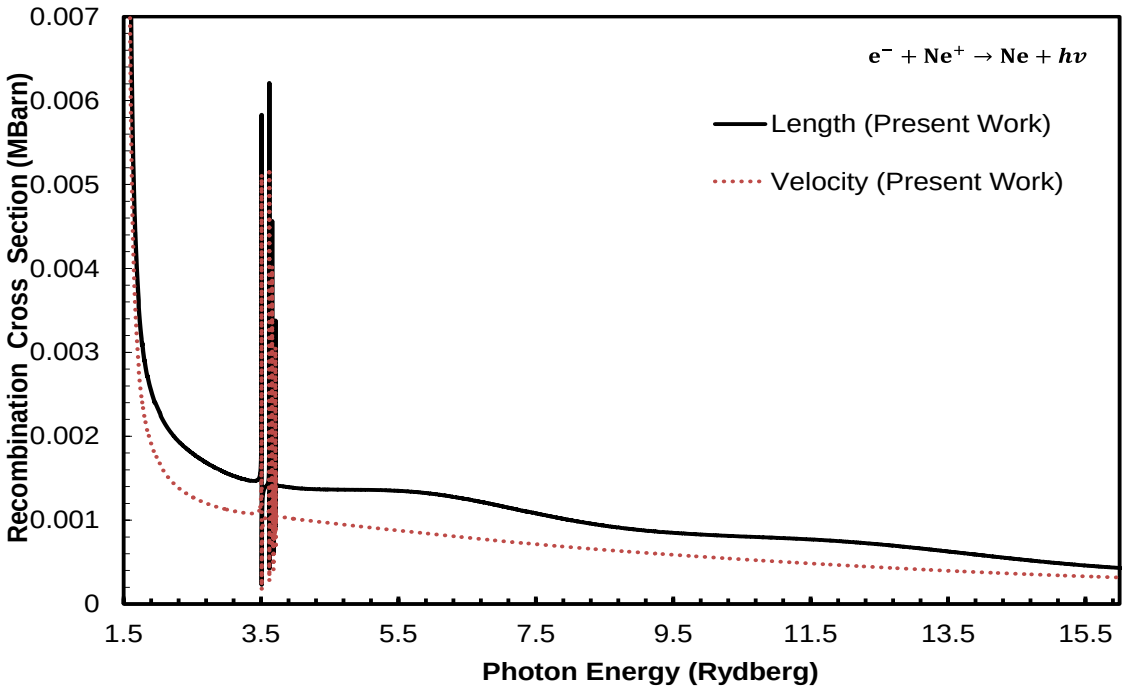

Figure (5) : Total recombination cross section of $(e^- + Ne^+ \rightarrow Ne + hv)$ in the length and velocity gauge.

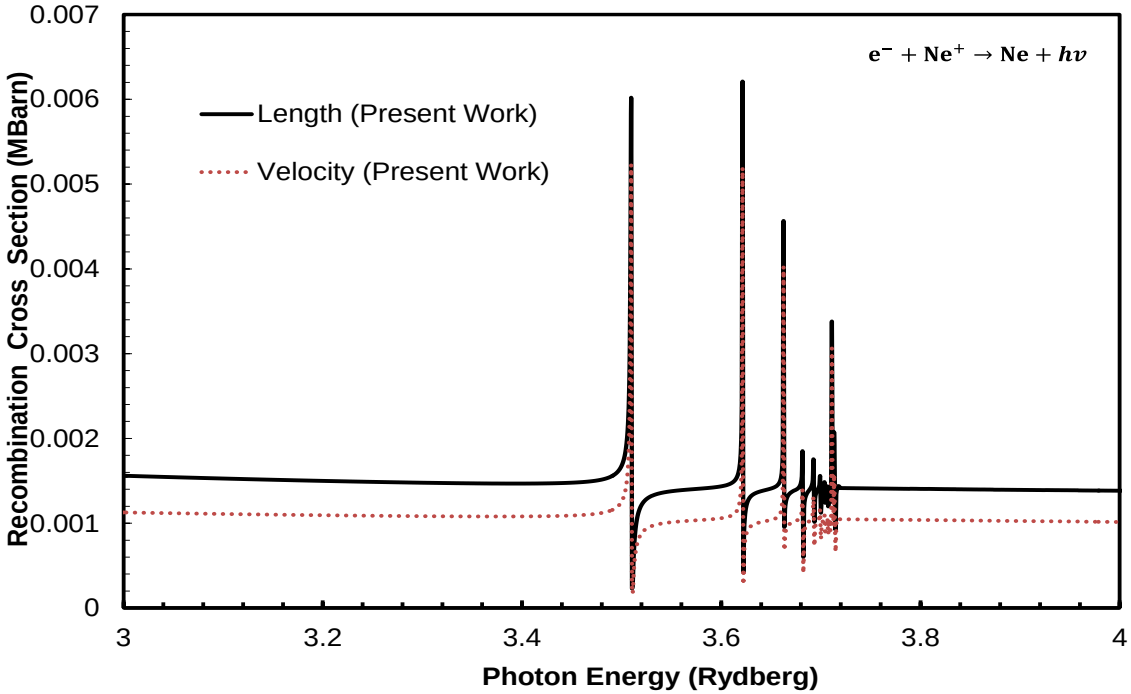

Figure (6) : Expansion of figure (5).

4. Conclusion

Energy levels,the absorption oscillator strength , radiative rate for an allowed transition and line strength for E1 transition,as well as the Photoionization and electron-ion recombination of He and Ne rare gas atoms are investigated using the fully relativistic R-matrix method .These processes are fundamental atomic processes in astrophysical plasmas. In most existing astrophysical models these atomic data are from methods that do not adequately consider the level of complexity attributable to the large number of autoionizing resonances that manifest themselves in the photoionization cross-sections and, consequently, in the inverse process of (electron-ion) recombination.The Dirac Atomic R-matrix Code has been used to handle bound states , photoionization, radiative recombination and other radiative processes . A relativistic atomic structure program GRASP is used to obtain bound orbitals from which the target ions are constructed in Dirac atomic R-matrix code DARC. Further relativistic contributions to the atomic states due to Breit interactions are added by diagonalizing the Dirac-Coulomb-Breit Hamiltonian matrix.The dominant quantum electrodynamic contibutions have also been included as a perturbation.Calculations have been performed on He and Ne rare gas atomic systems where the results obtained include the energy of levels ,the oscillator strength (f_{ij}) , radiative rates (A_{ji}),line strength (S_{ij}) for an electric dipole allowed transitions,Photoionization and Photo-recombination cross-sections.The results obtined in this paper are in good agreement with the results of others

References

[1] J.B.West, J. Phys. B 34 (2001) R45.
[2] M.J. Seaton, J. Phys. B 20 (1987) 6363.
[3] K.A.Berrington et.al., J. Phys. B20 (1987) 6379.
[4] O.Zatsarinny, Comput. Phys. Comm.,174 (2006) 273–356.
[5] A. Einstein. Ann. Phys. (Leipzig), **17**, 132 (1905).
[6] H. Hall. Rev. Mod. Phys. **8**, 358 (1936).
[7] H.A.Bethe and E.E.Salpeter, Quantum mechanics of one and two-electron atoms. Springer-Verlag, Berlin. 1958. p. 299.
[8] U. Fano and J.W. Cooper. Rev. Mod. Phys. 40, 441 (1968).
[9] A.F. Starace. Handbuch der Physik. Vol. 31. Edited by W. Mehlhorn, Springer-Verlag, Berlin. 1982. pp. 1–121.
[10] R.McWhirter and H.Summers, Applied Atomic Collision Physics (Academic, New York, 1983).
[11] E. I. Moses, R. N. Boyd, B. A. Remington, C. J. Keane, and R. Al Ayat, Phys. Plasmas 16, 041006 (2009).
[12] V. Schmidt, Rep. Prog. Phys. 55, 1483 (1992).
[13] H. S. Chakraborty, PRAMANA journal of physics,Vol.50,No.6, pp. 607(1998).
[14] N.S.Scott, Comput. Phys. Comm., 180 (2009) 2424–2449.
[15] P.G. Burke, K.A. Berrington (Eds.), Atomic and Molecular Processes and R-Matrix Approach, IOP Publishing, Bristol, 1993.
[16] P.G. Burke, C.J. Noble, V.M. Burke, Adv. At. Mol. Opt. Phys. 54 (2007) 237.
[17] E.P. Wigner, Phys. Rev. 70 (1946) 15.
[18] E.P. Wigner, Phys. Rev. 70 (1946) 606.
[19] P.G. Burke, Computational Physics, Inst. Phys. and Phys. Soc., London(1970) 9 .
[20] D.C.S. Allison, Comput. Phys. Comm. 1 (1969) 16.
[21] P.G. Burke, Comput. Phys. Comm. 1 (1969) 241.
[22] A. Hibbert, Comput. Phys. Comm. 1 (1970) 359.
[23] W.D. Robb, Comput. Phys. Comm. 1 (1970) 457.

[24] W.D. Robb, The calculation of atomic properties, Ph.D. thesis, The Queen's University of Belfast, 1971.
[25] K.A. Berrington, P.G. Burke, J.J. Chang, A.T. Chivers, W.D. Robb, K.T. Taylor,Comput. Phys. Comm. 8 (1974) 149.
[26] K.A. Berrington, P.G. Burke, M. Le Dourneuf, W.D. Robb, K.T. Taylor, V.K. Lan, Comput. Phys. Comm. 14 (1978) 367.
[27] N.S. Scott, K.T. Taylor, Comput. Phys. Comm. 25 (1982) 347.
[28] P.G. Burke, V.M. Burke, N.S. Scott, Comput. Phys. Comm. 69 (1992) 76.
[29] K.A. Berrington, W.B. Eissner, P.H. Norrington, Comput. Phys. Comm. 92 (1995) 290.
[30] K.A. Berrington, P.G. Burke, K. Butler, M.J. Seaton, P.J. Storey, K.T. Taylor, Yu. Yan, J. Phys. B: At. Mol. Phys. 20 (1987) 6379.
[31] M.J. Seaton, J. Phys. B: At. Mol. Phys. 20 (1987) 6363.
[32] D.G. Hummer, K.A. Berrington, W. Eissner, A.K. Pradhan, H.E. Saraph, J.A. Tully, Astron. Astrophys. 279 (1993) 298.
[33] P.G.Burke, A.Hibbert and W.D.Robb , J. Phys. B 4 (1971)153.
[34] P.H. Norrington and I.P.Grant, J. Phys. B 20 (1987)4869.
[35] W.P. Wijesundera et.al., J. Phys. B 24 (1991)1803.
[36] P.H. Norrington, I.P. Grant, online at http://www.am.qub.ac.uk/DARC/.
[37] P.G. Burke, A.Hibbert and W.D.Robb, J. Phys. B: At. Mol. Phys. 4 (1971) 153.
[38] J.J.Chang, J. Phys. B: At. Mol Phys. 8 (1975) 2327.
[39] S.N.Nahar, The Astrophysical Journal Supplement Series, 156(2005)93–103.
[40] S. N. Nahar, Atomic Data and Nuclear Data Tables 80, (2002) 205–234.
[41] K.M. Aggarwala and F.P. Keenan, Eur. Phys. J. D 46, (2008) 205–213.
[42] J.B.West and G.V.Marr , Proc. R. Soc. London Ser. A 349 (1976) 397.
[43] G.W.Erickson , J. Phys. Chem. Ref. Data 6 (1977) 831.
[44] N.R.Badnell, Comput. Phys. Comm. 182 (2011) 1528-1535.
[45] C.E.Moore , *Circular NBS* 467 (1949) vol 1.
[46] S.N.Nahar,New Astronomy,15(2010)417-426.
[47] A.Hibbert and M.P.Scott, J. Phys. B: At. Mol. *Phys.* 27 (1994) 1315.
[48] J.J. Yeh and I.Lindau, *Atomic Data and Nuclear Data Tables*, **32**, 1-155 (1985).
[49] D.A.Verner and D.G.Yakovlev,A&AS, 109(1995)125.

ألتاين ألضوئي , أعادة المزج بين ألالكترون وألايون والعمليات ألاشعاعيه لانظمة الهليوم والنيون الذرية باستخدام ألطريقة ألنسبية لمصفوفة ألبعد لديراك

عقيل هاشم حسين علاء عبد الحسن خلف فلحي عبد ألحسن علي
قسم الفيزياء / كلية العلوم / جامعة البصرة
akeel_hashem74@yahoo.Com

ألخلاصة

تم دراسة ألتاين ألضوئي , أعادة المزج بين ألالكترون وألايون والعمليات ألاشعاعيه لانظمة الهليوم والنيون الذرية باستخدام ألطريقة ألنسبية لمصفوفة ألبعد لديراك.هذه العمليات هي عمليات ذرية أساسيه في فيزياء البلازما . في اكثر النماذج سابقا هذه المقادير الذرية لا تمثل بصورة كافية مستوى المشاركة لعدد كبير من عمليات ألتأين الرنيني التلقائي الموضح في مقاطع التاين الضوئي واعادة المزج بين الالكترون والايون .ان ألطريقة ألنسبية لمصفوفة ألبعد لديراك امتدت وتوسعت من عمليات استطارة الكترون الطاقة الواطئه لتشمل الحالات المقيده ,ألتاين الضوئي واعادة المزج.أن الدوال الموجية للمدارات في الحسابات النسبية لمصفوفة البعد لديراك يتم الحصول عليها من طريقة ديراك–فوك المتعددة المساهمة وذلك باستخدام البرنامج الدولي(GRASP). حيث في هذه الطريقة فان دالة الحالة الذرية تقرب بواسطة المزج الخطي لدوال تشكيل الحالة ذات نفس التناظر.أن دوال تشكيل الحالة هي حاصل ضرب غير متناظر لمجموعة مشتركة من المدارات المتعامدة–العيارية والتي مجموعها تشكل دوال اساسية للمؤثر الهاملتوني لديراك–كولوم .هذة الدوال ألاساسية تستخدم لايجاد دوال المدارات المقيده الداخلة بتركيب ايون الهدف والتي تستخدم بالحسابات باستخدام البرنامج (DARC).تم اضافة تاثيرات نسبية أضافية للحالات ألذرية طبقا لتفاعلات بريت وذلك بجعل المصفوفة الهاملتونية لديراك–كولوم–بريت مصفوفة قطرية.كذلك تم أضافة ألتأثير ألكهرومغناطيسي ألكمي ألمؤثر بصورة قوية كحد تصحيح للمؤثر ألهاملتوني .أن الحسابات انجزت على أنظمة الهليوم والنيون ألذرية حيث تم الحصول على اتفاق جيد بين النتائج في هذا البحث مع نتائج الباحثين الاخرين .

كلمات مفتاحية : ألتاين ألضوئي , أعادة مزج ألكترون– أيون , معادلة ديراك , طريقة مصفوفة البعد النسبية